Automatic Generation Control Using an Actor-Critic based Adaptive PID controller

Nikhil Nair
NITK, Surathkal

Manav Singhal
NITK, Surathkal

Suraj Kulkarni
NITK, Surathkal

Rasananda Muduli
NITK, Surathkal

Debashisha Jena
NITK, Surathkal

***Abstract*—Automatic Generation Control (AGC) is critical for providing quality electrical energy. In this paper, we present an Actor-Critic Reinforcement Learning (RL) based Adaptive Proportional-Integral-Derivative (PID) controller. The performance of model-based control methods relies on the accuracy of the available plant model. There is a need for adaptive controllers that, for the most part, work independently of the system configuration. The PID controller parameters are updated through an actor-critic policy in real-time. This actor-critic policy is implemented as a single RBF kernel implemented as a neural network. The input to the RBF kernel is the Area Control Error (ACE) after being passed through a state converter. The kernel outputs the updated parameters of the PID controller. We employ the gradient descent method based on the Temporal Difference (TD) error performance index to update the neural network's weights. The neural network and the kernel are continually updated, making the controller robust and adaptive. Numerical simulations were performed, and the controller's performance was recorded and compared to a traditional PID controller.**

***Index Terms*—PID Controller, Automatic Generation Control, Reinforcement Learning, Adaptive Control**

I. Introduction

Power networks are responsible for transporting electricity across large geographical regions. They are complex infrastructures on which modern life critically depends. Demand variations, renewable energy integration, and high voltage network technology are real challenges for human operators when optimizing electricity transportation to avoid blackouts.

Power systems maintain an equilibrium between power generated and load to ensure stable operation. This is in order to maintain frequency within the necessary limits. In real-time, there are persistent load disturbances. This affects the balance between generation and load, which in turn impacts system frequency and hence the security of the entire power system. Maintaining constant frequency and scheduled power is critical for industrial and commercial use. To achieve this, Automatic Generation Control (AGC) is employed to ensure reliable and quality supply of electric power.

AGC has been implemented in various ways. The most common and widely implemented controller is the traditional Proportional (PI) controller. Controller techniques using optimal control theory allow designing a control system based on a certain performance criterion such as Area Control Error(ACE). This was first presented in [1]. In previous works AGCs with a centralized control paradigm were employed [2], [3], [4], [5]. In [2], many control strategies have been proposed based on the kind of load disturbances. In [3] they proposed a proportional controller, disregarding the steady-state requirements and compensation of load disturbances. The major disadvantages of using a centralized strategy include the complexity of sharing information between areas, storage issues, and increased computation. To counter these problems, a decentralized paradigm was proposed and can be found in [6], [7], [8], [9], [10], [11], [12]. In our implementation, we go for a decentralized approach with a controller for each area. In [13], discrete mode AGC of an interconnected power system with a novel ACE based on tie-line power deviation, frequency deviation, time error, and inevitable changes.

In many of these methods, non-linear systems are approximated linear based on specific system properties. The application of neural networks allows for better ways to deal with non-linear control problems and non-linear operating ranges. The applications of neural networks in power system control are witnessed in [14], [15], [16], [17], [18], [19]. Test results from [15] reveal that neural network-based AGC implementation had a significant improvement over the modern AGC implementations. In fuzzy logic control, instead of deriving a controller via modeling the controlled process quantitatively and mathematically, the method tries to establish the controller directly from the operators who are controlling the process [20], [21], [22]. Genetic Algorithms (GA) are widely used to solve complex non-linear optimization problems, especially in the field of AGCs [23], [24], [25], [26], [27], [28], [29], [30]. Modern Reinforcement Learning techniques can be used to design AGCs, offering key advantages like modular independence and flexibility in specifying control objectives.

This paper is organized as follows. Section 2 presents our methodology, which includes the power system model, the structure of the velocity type PID controller, the Actor-Critic network with the RBF kernel, and our implementation for the same. The following section presents our results of the proposed approach. Finally, concluding remarks are included in Section 4.

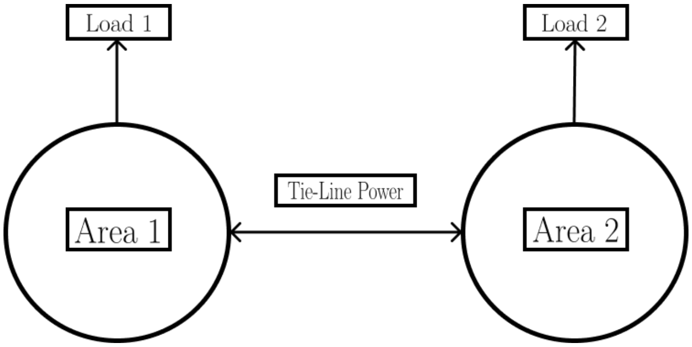

Fig. 1. Two interconnected control areas

II. Methodology

A. Power System Model

1) Automatic Generation Control: Controlling frequency is as important, if not more important, than controlling voltage. Since motor speed is directly proportional to frequency, variation in frequency leads to variation in the speed of flour mills, clocks, and paper printing machines. Power generation systems require a controller to control generation to offset the variation in load demand.

Two control loops control the frequency of the power system, primary and secondary [31].

- The primary control loop prevents instant variations in the frequency. It typically gives rise to the steady-state error.
- Steady-state error in frequency is regulated using the secondary control, also termed automatic generation control (AGC).

Thus to summarize, AGC is employed to:

- regulate steady-state frequency to its nominal value
- maintain tie-line power flow to its defined value
- reduce settling time and overshoot

A linear equation called area control error (ACE) is used to accomplish these objectives, which is associated with two main focal variables, frequency variance and tie-line power exchange. In the event of any load disturbances, AGC uses ACE as a reference signal and sets it to zero.

$$ACE = \triangle P_{tie} + \beta_{area} \triangle f \tag{1}$$

where $\triangle P_{tie}$ is the tie-line power and the constant β_{area} is called the frequency bias constant.
This approach aims to be flexible by keeping $\triangle P_{tie}$ and $\triangle f$ within a suitable band. The task of the AGC is to achieve maximum economy and constant frequency by distributing the load among the subsystems effectively.

2) Two Area Power System: Modern power systems consist of smaller isolated areas that are interconnected using transmission lines called tie-lines (Fig. 1). These lines share power between the two areas. Each area has its governor, turbine generator, and plant. A power system with many generators and loads can be divided into subareas in which generators are tightly coupled together to form a coherent group. All the generators respond in unison to changes in load or speed changer settings. Such a coherent area is called a control area in which the frequency is the same throughout in static and dynamic conditions.

3) Modeling of Two Area Power System: Fig. 2 shows the block diagram representation of the Two Area Power System

4) State Space Model of the System: Consider the system in the state variable form:

$$\dot{X}(t) = Ax(t) + Bu(t) \tag{2}$$

$$Y(t) = Cx(t) \tag{3}$$

We obtain the matrices A, B and C as follows:

$$[A] = \begin{bmatrix} \frac{-1}{T_P} & \frac{K_P}{T_P} & 0 & \frac{-K_P}{T_P} & 0 & 0 & 0 \\ 0 & \frac{-1}{T_t} & \frac{1}{T_t} & 0 & 0 & 0 & 0 \\ \frac{-1}{R_{Tg}} & 0 & \frac{-1}{T_g} & 0 & 0 & 0 & 0 \\ 2\pi T_{12} & 0 & 0 & 0 & -2\pi T_{12} & 0 & 0 \\ 0 & 0 & 0 & \frac{-K_P a_{12}}{T_P} & \frac{-1}{T_P} & \frac{K_p}{T_P} & 0 \\ 0 & 0 & 0 & 0 & 0 & \frac{-1}{T_t} & \frac{1}{T_t} \\ 0 & 0 & 0 & 0 & \frac{-1}{R_{Tg}} & \frac{1}{T_g} & \frac{-1}{T_g} \end{bmatrix}$$

$$[B] = \begin{bmatrix} \frac{-K_P}{T_P} & 0 & 0 & 0 \\ 0 & 0 & 0 & 0 \\ 0 & 0 & \frac{1}{T_g} & 0 \\ 0 & 0 & 0 & 0 \\ 0 & 0 & 0 & 0 \\ 0 & 0 & 0 & 0 \\ 0 & \frac{-K_P}{T_P} & 0 & \frac{1}{T_g} \end{bmatrix}$$

$$[C] = \begin{bmatrix} \beta_1 & 0 & 0 & 1 & 0 & 0 & 0 \\ 0 & 0 & 0 & 1 & \beta_2 & 0 & 0 \\ 0 & 0 & 0 & 1 & 0 & 0 & 0 \\ 1 & 0 & 0 & 0 & 0 & 0 & 0 \\ 0 & 0 & 0 & 0 & 1 & 0 & 0 \end{bmatrix}$$

where,

$$[X] = \begin{bmatrix} x1 \\ x2 \\ x3 \\ x4 \\ x5 \\ x6 \\ x7 \end{bmatrix} = \begin{bmatrix} \triangle f_1 \\ \triangle P_{g1} \\ \triangle P_{hA} \\ \triangle f_2 \\ \triangle P_{g2} \\ \triangle P_{h2} \\ \triangle P_{tie} \end{bmatrix}$$

5) Discretization: For numerical computing, discretization of the state space model is required. Discretization is concerned with transforming continuous differential equations into discrete difference equations [32]. The following continuous time state-space model:

$$\dot{x} = Ax(t) + Bu(t) \tag{4}$$

$$y(t) = Cx(t) + Du(t) \tag{5}$$

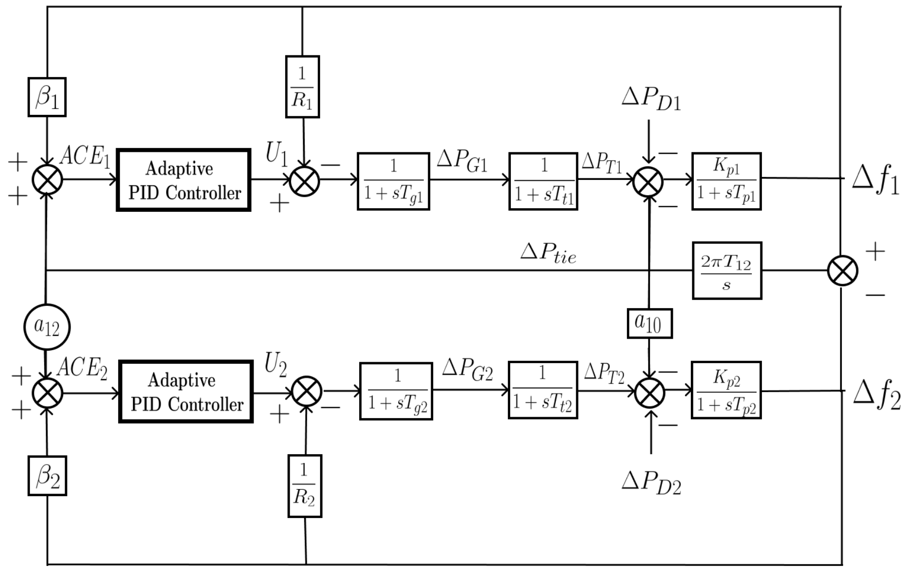

Fig. 2. Two area power system

can be discretized, assuming zero-order hold for the input u, to

$$x[k+1] = A_d x[k] + B_d u[k] \tag{6}$$

$$y[k] = C_d x[k] \tag{7}$$

where,

$$A_d = e^{AT} = \mathcal{L}^{-1}\{(sI - A)^{-1}\}_{t-T} \tag{8}$$

$$B_d = (\int_{\tau=0}^{T} e^{A\tau}\, d\tau)B = A^{-1}(A_d - I)B, \text{if A is non-singular.} \tag{9}$$

$$C_d = C \tag{10}$$

B. The structure of the Velocity Type PID controller

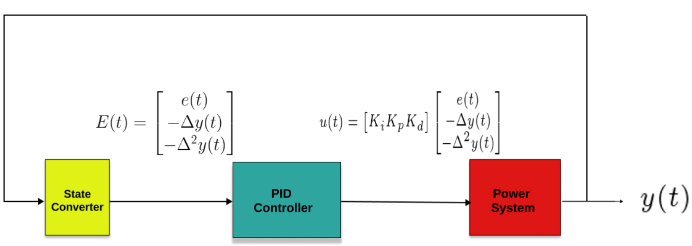

Fig. 3. PID Controller Block Diagram

Even today, most industries use standard PID controllers because they are simple, easy, and clear to implement. The distinct characteristic of a PID controller is that it uses three control terms, Proportional (P), Integral (I), and Derivative (D), on the error signal for control.

The control signal u(t) of the PID controller is the sum of three terms:

$$u(t) = K_p e(t) + K_i \int_0^{\tau} e(t) d\tau + K_d \frac{de}{dt} \tag{11}$$

where,

$e(t)$: Error Signal

K_p : Proportional Constant

K_i : Integral Constant

K_d : Derivative Constant

1) Controller Actions:

- Proportional: The error signal is amplified by a gain. The speed of response is directly proportional to the gain.
- Integral: It is used to remove the steady-state error. However, this control action increases the overshoot and makes the system unstable.
- Derivative: It is used to better the transient response by reducing overshoot.

2) Digital PID controller: To implement PID control on a digital computer, we convert the continuous-time equation (11) into a discrete form. To do this, we approximate integral and derivative using finite differences.

$$u(t) = K_p e(t) + K_i \int_0^{\tau} e(t) d\tau + K_d \frac{de}{dt} \tag{12}$$

$$\int_0^{\tau} e(t) d\tau : \sum_{k=1}^{n} Te(Tk) \tag{13}$$

$$\frac{de}{dt} : \frac{e(nT) - e((n-1)T)}{T} \tag{14}$$

$$u_n = K_p e_n + K_i \sum_{k=1}^{n} e_n + K_d \frac{e_n - e_{n-1}}{T} \tag{15}$$

This is known as the position form of the discrete PID controller.

3) Velocity form of the digital PID Controller: For the design of our PID controller, we went with a velocity-type PID controller, which can reduce the derivative kick. The PID controller design was inspired by [3].

From the position form we can write:

$$u_n = K_p e_n + K_i \sum_{k=1}^{n} e_n + K_d \frac{e_n - e_{n-1}}{T} \tag{16}$$

For a previous time step we can write:

$$u_{n-1} = K_p e_{n-1} + K_i \sum_{k=1}^{n-1} e_{n-1} + K_d \frac{e_{n-1} - e_{n-2}}{T} \tag{17}$$

Subtracting these two equations we get our PID controller in Velocity form:

$$u_n = u_{n-1} + K_p[e_{n-1} - e_{n-1}] + K_i e_n + K_d \frac{e_n - 2e_{n-1} + e_{n-2}}{T} \tag{18}$$

4) Controller Design: For the power system we design a velocity-type PID controller like:

$$u_t = u_{t-1} + K_i e_t - K_p \Delta y(t) - K_d \Delta^2 y(t) \tag{19}$$

where,

$$y(t) : \text{System Output}$$

$$y_d(t) : \text{reference signal}$$

$$e(t) : y_d(t) - y(t)$$

$$\Delta y(t) : y(t) - y(t-1)$$

$$\Delta^2 y(t) : y(t) - 2y(t-1) + y(t+2)$$

The error signal is defined as follows:

$$E(t) = [e(t), -\Delta y(t), -\Delta^2 y(t)]^T \tag{20}$$

Thus, the controller can be rewritten in the following manner:

$$u(t) - u(t-1) = K(t)E(t) \tag{21}$$

$$\Delta u(t) = K(t)E(t) \tag{22}$$

where $K(t)$ is a vector of the control parameters and is the output of the adaptive controller.

$$K(t) = [K_i(t), K_p(t), K_d(t)]$$

C. Actor-Critic network with the Radial Basis Function (RBF) kernel

1) Reinforcement Learning: Our model is a Reinforcement Learning (RL) based algorithm[33]. The Value function helps to measure how rewarding a state is using the prediction of the future rewards from that state.

In our method, it is defined as:

$$V(t) = \sum_{i=t}^{\infty} \gamma^{i-t} r(x(i), u(i)) \tag{23}$$

with $0 < \gamma \leq 1$ a discount factor and $u(t)$ control signal.

Function $r(x(i), u(i))$ is known as reinforcement signal which helps to determine the reward obtained for immediate and future timesteps.

Avoiding the infinite summation in the value function evaluation for future timesteps, we use the control signal to our advantage to obtain the value function as:

$$V(t) = r(x(t), u(t)) + \gamma V(t+1), V(0) = 0 \tag{24}$$

[Bellman Equation]

Based on the Bellman equation obtained, a temporal difference error (TD error) is calculated based on the difference at either ends of using reward and value function as follows:

$$\delta_{TD}(t) = r(x(t), u(t)) + \gamma V(t+1) - V(t) \tag{25}$$

In an ideal case of optimal control policy, the Bellman equation will hold and the TD error will be zero.

2) Radial Basis Function: Radial Basis Function (RBF) [34] is an artificial neural network with an input layer, a hidden layer, and an output layer. The hidden layers have hidden neurons, with the activation functions of the neurons being a Gaussian function. For every input vector, a hidden layer generates a signal based on which a response is outputted. The reason for favoring RBF networks include their simple structure, parameters convergence, and their adequate learning. Using function mappings, they can excel at identifying parameters.

RBFs help in faster convergence compared to Multi-Layer Perceptrons (MLP). Hence, it is preferred over MLP when dealing with low-dimensional data, and the output is directly correlated to the input vector components. They are universal approximators contributing to the robustness our model aims to achieve.

The input layer consists of available process measurements and system states in our method. The output of the RBF is shared jointly by the Actor and Critic. Using the weighted sum of the function values related to the units in the hidden layers, we obtain the control signal $u(t)$ and our value function [35].

The hidden layer encompasses $\phi_j(t)$ which is the vector containing the elements $[\phi_1(t), \cdots, \phi_h(t)]$, where h is the number of the hidden units. As discussed prior, the kernel function for the RBF network's hidden layer is the Gaussian function. Hence the output $\phi(t)$ is denoted as follows:

$$\phi_j(t) = e(-\frac{\|\theta(t) - \mu_j(t)\|^2}{2\sigma_j^2(t)}), j = 1, 2, 3..., h \tag{26}$$

where, μ_j and σ_j are the center vector and width scalar of the unit, respectively. The center vector ($\mu_j(t)$) which is the mean values is defined as follows:

$$\mu_j(t) := [\mu_{1j}, \mu_{2j}, \mu_{3j}]^T$$

The output layer yields our K values for the PID controller which becomes our Actor values while the value function outputted caters to the Critic[35].

Actor:

$$K_{P,I,D}(t) = \sum_{j=1}^{h} w_j^{P,I,D}(t)\phi_j(t) \tag{27}$$

with the weights w_{nj} between the jth hidden unit and output layer of the Actor.

Critic:

$$V(t) = \sum_{j=1}^{h} v_j(t)\phi_j(t) \tag{28}$$

where $v_j(t)$ denotes the weight between the jth hidden unit and output layer of the Critic.

The various weights for each of the neurons are trained using gradient-based learning, thus obtaining the adaptive updating of our PID parameters.

Our reinforcement signal for our RL based algorithm is defined as follows:

$$r(x(t), u(t)) := \frac{1}{2}(y_d(t+1) - y(t+1))^2 \tag{29}$$

which indicates the difference between predictive performance ($y(t+1)$) and reference value ($y_d(t+1)$). This could be mapped to a simple mean squared loss.

The TD error in our case then becomes:

$$\delta_{TD}(t) = \frac{1}{2}(y_d(t+1) - y(t+1))^2 + \gamma V(t+1) - V(t) \tag{30}$$

This TD error involves the immediate reward clubbed with future rewards being incorporated into the current time decision step.

While the cost function is defined as follows:

$$J(t) = \frac{1}{2}\delta_{TD}^2(t) \tag{31}$$

The update function is defined as follows[35]:

$$w_j^P(t+1) = w_j^P(t) - \alpha_w \frac{\partial J(t)}{\partial w_j^P(t)} \tag{32}$$

The update rule for the weights of the critic is[35]:

$$v_j(t+1) = v_j(t) + \alpha_v \delta_{TD}(t)\phi_t(t) \tag{33}$$

where, α_v is the learning rate.

The centers of the hidden units in the hidden layer are updated as follows[35]:

$$\mu_{ij}(t+1) = \mu_{ij} + \alpha_u \delta_{TD}(t) v_j(t)\phi_j(t) \frac{\psi_i(t) - \mu_{ij}(t)}{\sigma_j^2(t)} \tag{34}$$

while, the widths of the hidden units are updated as follows[35]:

$$\sigma_j(t+1) = \sigma_j + \alpha_\sigma \delta_{TD}(t) v_j(t)\phi_j(t) \frac{\|\psi_i(t) - \sigma_j(t)\|^2}{\sigma_j^3(t)} \tag{35}$$

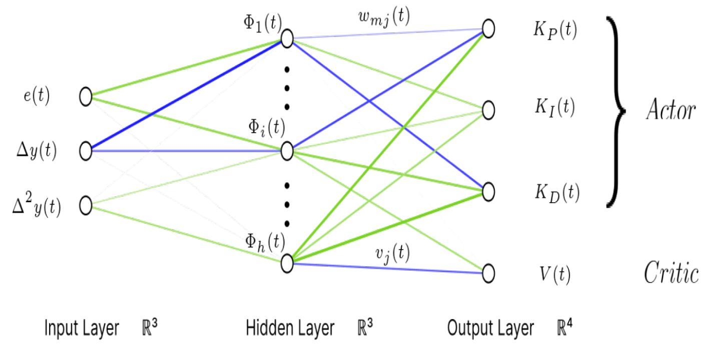

Fig. 4. Actor-Critic based RBF Kernel

D. Implementation

Algorithm 1 Adaptive PID controller using RBF Kernel

Require: Initialize Power System and Controllers
1. Set Control Signal $u(t) = 0$
2. Initialize the parameters such as w , v, μ and σ matrices
3. Set the values for the user specified learning rates α_w , α_v , α_μ and α_σ .
4. Set $t_0 = 0$
5. y_{t-1}, y_{t-2} and $y_{t-3} \leftarrow 0$
6. $X_t \leftarrow x$
7. **while** $t_i <= Runtime$ **do**
8. Calculate error signal:
$$E(t) = [e(t), -\Delta y(t), -\Delta^2 y(t)]$$
9. Send error signal to controllers and update K values
10. Send control signal:
$$u_t = u_{t-1} + K_i e_t - K_p \Delta y(t) - K_d \Delta^2 y(t)$$
11. Update weights of RBF kernel
12. Update y_{t-1} , y_{t-2} and y_{t-3}
13. **end while**

RESULTS

Numerical simulations were performed by running the power system model along with the two controllers - The adaptive RBF-based PID controller and a PSO-tuned PID controller. Fig. 5 shows the load disturbance that was provided to the system. The ACE signal in the two areas are shown in Fig. 6 and Fig. 7 between 100-200 seconds.

The simulations suggest that the adaptive controller performs better than the PSO-tuned PID controller for a given load disturbance as well as varying load disturbances, with a lower overshoot. These observations were quantified using four metrics, ITSE, IAE, ITAE, and ISE, calculated on the ACE (Eq: (1)) values.

$$ITSE = \int_0^T t[ACE^2]dt \tag{36}$$

$$IAE = \int_0^T |ACE|dt \tag{37}$$

$$ITAE = \int_0^T t[|ACE|]dt \tag{38}$$

$$ISE = \int_0^T [ACE^2]dt \tag{39}$$

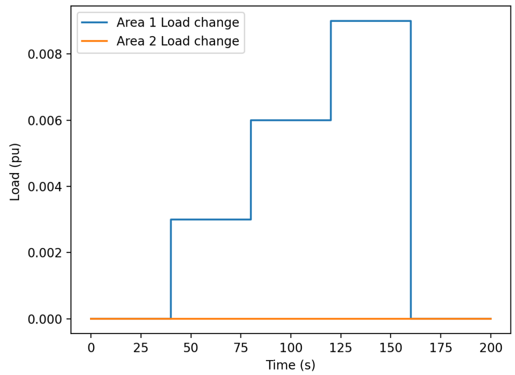

Fig. 5. Load Disturbance graph for Area 1 and Area 2

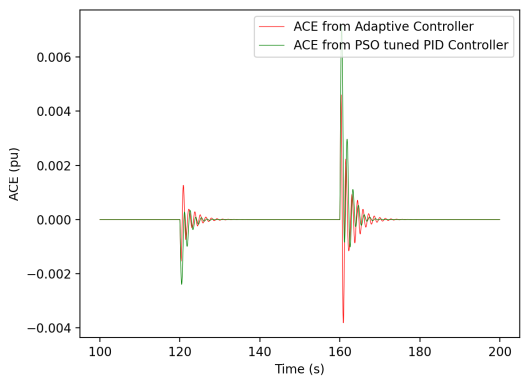

Fig. 6. ACE graph for Area 1

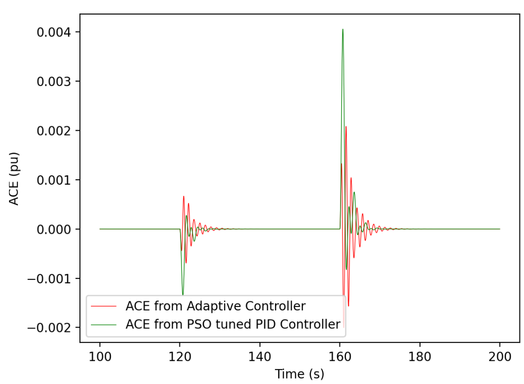

Fig. 7. ACE graph for Area 2

Conclusions

This paper proposes a novel adaptive PID controller using an Actor-Critic network for a two-area power system. ACE was used as the input signal, which was fed to the RBF network. The Actor and the Critic shared the hidden layer of the RBF network. The Actor provided the K-values, which were then integrated with a PID controller. This PID tuning occurred in an on-line manner. The Critic generates the value function, which, along with the TD error, was used to update the network parameters through gradient descent. Numerical simulations were given to indicate the efficiency and feasibility of the proposed scheme for AGC. In the future, different variations of Actor-Critic networks can be explored.

TABLE I
Comparison between Adaptive PID Controller and PSO-tuned PID Controller

Performance Metrics	**Adaptive PID controller**	**PSO-tuned PID controller**
ISTE	0.00339	0.00711
IAE	0.02213	0.02393
ITAE	2.71149	2.90879
ISE	2.40742e-05	5.05659e-05

Acknowledgment

This work was done as the Bachelors Major Project of Nikhil Nair, Manav Singhal and Suraj Kulkarni. We would also like to thank Dr. Tukaram Moger for his inputs.

References

[1] C. E. Fosha and O. I. Elgerd, "The megawatt-frequency control problem: A new approach via optimal control theory," *IEEE Transactions on Power Apparatus and Systems*, no. 4, pp. 563–577, 1970.

[2] G. Quazza, "Noninteracting controls of interconnected electric power systems," *IEEE Transactions on Power Apparatus and Systems*, no. 7, pp. 727–741, 1966.

[3] O. I. Elgerd and C. E. Fosha, "Optimum megawatt-frequency control of multiarea electric energy systems," *IEEE transactions on power apparatus and systems*, no. 4, pp. 556–563, 1970.

[4] C. E. Fosha and O. I. Elgerd, "The megawatt-frequency control problem: A new approach via optimal control theory," *IEEE Transactions on Power Apparatus and Systems*, no. 4, pp. 563–577, 1970.

[5] M. Aldeen and H. Trinh, "Load-frequency control of interconnected power systems via constrained feedback control schemes," *Computers & electrical engineering*, vol. 20, no. 1, pp. 71–88, 1994.

[6] H. Kawabata and M. Kido, "A decentralized scheme of load frequency control of power system," *Electrical Engineering in Japan*, vol. 102, no. 4, pp. 100–106, 1982.

[7] A. Feliachi, "Optimal decentralized load frequency control," *IEEE transactions on power systems*, vol. 2, no. 2, pp. 379–385, 1987.

[8] M. S. Ćalović, "Automatic generation control: Decentralized area-wise optimal solution," *Electric power systems research*, vol. 7, no. 2, pp. 115–139, 1984.

[9] M. Aldeen and J. Marsh, "Observability, controllability and decentralized control of interconnected power systems," *Computers & electrical engineering*, vol. 16, no. 4, pp. 207–220, 1990.

[10] M. Aldeen, "Interaction modelling approach to distributed control with application to power systems," *International Journal of Control*, vol. 53, no. 5, pp. 1035–1054, 1991.

[11] T. Yang, H. Cimen, and Q. Zhu, "Decentralised load-frequency controller design based on structured singular values," *IEE Proceedings-Generation, Transmission and Distribution*, vol. 145, no. 1, pp. 7–14, 1998.

[12] T. Yang, Z. Ding, and H. Yu, "Decentralised power system load frequency control beyond the limit of diagonal dominance," *International journal of electrical power & energy systems*, vol. 24, no. 3, pp. 173–184, 2002.

[13] M. Kothari, J. Nanda, D. Kothari, and D. Das, "Discrete-mode automatic generation control of a two-area reheat thermal system with new area control error," *IEEE Transactions on power systems*, vol. 4, no. 2, pp. 730–738, 1989.

[14] F. Beaufays, Y. Abdel-Magid, and B. Widrow, "Application of neural networks to load-frequency control in power systems," *Neural Networks*, vol. 7, no. 1, pp. 183–194, 1994.

[15] L. Douglas, T. Green, and R. A. Kramer, "New approaches to the agc nonconforming load problem," pp. 48–57, 1993.

[16] D. Chaturvedi, P. Satsangi, and P. Kalra, "Load frequency control: a generalised neural network approach," *International Journal of Electrical Power & Energy Systems*, vol. 21, no. 6, pp. 405–415, 1999.

[17] H. L. Z. A. Demiroren, Neslihan S. Sengor, "Automatic generation control by using ann technique," *Electric Power Components and Systems*, vol. 29, no. 10, pp. 883–896, 2001.

[18] H. Zeynelgil, A. Demiroren, and N. Sengor, "The application of ann technique to automatic generation control for multi-area power system," *International journal of electrical power & energy systems*, vol. 24, no. 5, pp. 345–354, 2002.

[19] T. I. Ahamed, P. N. Rao, and P. Sastry, "A reinforcement learning approach to automatic generation control," *Electric power systems research*, vol. 63, no. 1, pp. 9–26, 2002.

[20] C. Indulkar and B. Raj, "Application of fuzzy controller to automatic generation control," *Electric machines and power systems*, vol. 23, no. 2, pp. 209–220, 1995.

[21] A. E. Gegov and P. M. Frank, "Decomposition of multivariable systems for distributed fuzzy control," *Fuzzy Sets and Systems*, vol. 73, no. 3, pp. 329–340, 1995.

[22] J. Talaq and F. Al-Basri, "Adaptive fuzzy gain scheduling for load frequency control," *IEEE Transactions on power systems*, vol. 14, no. 1, pp. 145–150, 1999.

[23] Y. Karnavas and D. Papadopoulos, "Agc for autonomous power system using combined intelligent techniques," *Electric power systems research*, vol. 62, no. 3, pp. 225–239, 2002.

[24] Y. Abdel-Magid and M. Dawoud, "Optimal agc tuning with genetic algorithms," *Electric Power Systems Research*, vol. 38, no. 3, pp. 231–238, 1996.

[25] C. Chang, W. Fu, and F. Wen, "Load frequency control using genetic-algorithm based fuzzy gain scheduling of pi controllers," *Electric Machines and power systems*, vol. 26, no. 1, pp. 39–52, 1998.

[26] Z. Al-Hamouz and H. Al-Duwaish, "A new load frequency variable structure controller using genetic algorithms," *Electric Power Systems Research*, vol. 55, no. 1, pp. 1–6, 2000.

[27] A. Abdennour, "Adaptive optimal gain scheduling for the load frequency control problem," *Electric Power Components and Systems*, vol. 30, no. 1, pp. 45–56, 2002.

[28] Aditya, "Design of load frequency controllers using genetic algorithm for two area interconnected hydro power system," *Electric Power Components and Systems*, vol. 31, no. 1, pp. 81–94, 2003.

[29] D. Rerkpreedapong, A. Hasanovic, and A. Feliachi, "Robust load frequency control using genetic algorithms and linear matrix inequalities," *IEEE Transactions on Power Systems*, vol. 18, no. 2, pp. 855–861, 2003.

[30] S. Ghoshal, "Application of ga/ga-sa based fuzzy automatic generation control of a multi-area thermal generating system," *Electric Power Systems Research*, vol. 70, no. 2, pp. 115–127, 2004.

[31] K. Ullah, A. Basit, Z. Ullah, S. Aslam, and H. Herodotou, "Automatic generation control strategies in conventional and modern power systems: A comprehensive overview," *Energies*, vol. 14, no. 9, 2021.

[32] Z. Kowalczuk, "On discretization of continuous-time state-space models: a stable-normal approach," *IEEE Transactions on Circuits and Systems*, vol. 38, no. 12, pp. 1460–1477, 1991.

[33] R. S. Sutton and A. G. Barto, "Reinforcement learning: An introduction," 2018.

[34] D. Broomhead and D. Lowe, "Radial basis functions, multi-variable functional interpolation and adaptive networks," *ROYAL SIGNALS AND RADAR ESTABLISHMENT MALVERN (UNITED KINGDOM)*, vol. RSRE-MEMO-4148, 03 1988.

[35] Z. Guan and T. Yamamoto, "Design of a reinforcement learning pid controller," *2020 International Joint Conference on Neural Networks (IJCNN)*, pp. 1–6, 2020.

[]